Desalination and Water Treatment
www.deswater.com

doi: 10.1080/19443994.2015.1026282

57 (2016) 8839–8853
April

Taylor & Francis
Taylor & Francis Group

Adsorption of methylene blue onto coconut (*Cocos nucifera*) leaf: optimization, isotherm and kinetic studies

Ali H. Jawad[a,b,*], Ramlah Abd Rashid[a,b], Roweda M.A. Mahmuod[c], Mohd Azlan Mohd Ishak[a,b], Nur Nasulhah Kasim[a,b], Khudzir Ismail[a,b]

[a]*Coal and Biomass Energy Research Group, Faculty of Applied Sciences, Universiti Teknologi MARA, 40450 Shah Alam, Selangor, Malaysia, Tel. +60 49882571; emails: ahjm72@yahoo.com, ali288@perlis.uitm.edu.my (A.H. Jawad), Tel. +60 124872038; email: d_chemist@yahoo.com (R.A. Rashid), Tel. +60 49882027; email: azlanishak@perlis.uitm.edu.my (M.A.M. Ishak), Tel. +60 49882515; email: nurnasulhah@perlis.uitm.edu.my (N.N. Kasim), Tel. +60 355444562; email: khudzir@salam.uitm.edu.my (K. Ismail)*

[b]*Coal and Biomass Energy Research Group, Faculty of Applied Sciences, Universiti Teknologi MARA, Arau Campus, 02600 Arau, Perlis, Malaysia*

[c]*School of Quantitative Sciences, College of Arts and Science, Universiti Utara Malaysia, 06010 Sintok, Kedah, Malaysia, Tel. +60 1641616100; email: roweda.zwain@gmail.com*

Received 19 August 2014; Accepted 28 February 2015

ABSTRACT

Fallen coconut leaves (CLs) are agricultural wastes largely available in Malaysia. In this study, we utilized CLs as a low-cost adsorbent for adsorptive removal of methylene blue (MB), a cationic dye from aqueous solution. Response surface methodology was employed to investigate the effects of operational parameters on MB removal efficiency. The investigated variables included adsorbent dosage (0.5–1.5 g/L), initial MB concentration (10–50 mg/L), initial solution pH (4–10), and agitation time (5–45 min). The analysis of variance was incorporated to test the adequacy of the model. The highest MB removal efficiency was achieved by simultaneous interactions between adsorbent dosage with pH, adsorbent dosage with agitation time, and pH with agitation time. Other simultaneous interactions showed lower effects. The optimum adsorbent dosage, initial MB concentration, initial solution pH, and agitation time were 1.26 g/L, 19.01 mg/L, 8.65, and 5.00 min, respectively. Under optimal conditions, high removal efficiency for MB was observed as 86.38%, and the equilibrium adsorption isotherms and kinetics were investigated. The Langmuir, Freundlich, and Temkin models of adsorption were used to analyze the experimental data. Pseudo-first-order and pseudo-second-order models were also employed to analyze the kinetic data obtained at different MB initial concentrations. The adsorption kinetics closely followed the pseudo-second-order model. Based on the Langmuir model, the maximum adsorption capacity of MB on the CL surface was 112.35 mg/g at 27 ± 2°C.

Keywords: Adsorption; Methylene blue; Coconut leaves; Low-cost adsorbent; Optimization; Response surface methodology

*Corresponding author.

1. Introduction

Over the past decades, the discharge of dye effluents from textile, leather, paper, and plastic industries into water streams, aquifer systems, and the environment poses serious problems to many life forms. Removing dyes from the aquatic environment is extremely important from the health point of view because most of these dyes are toxic and cause allergy and skin irritation. Moreover, most of these dyes are mutagenic and carcinogenic [1–3]. Therefore, industrial effluents containing dyes should be treated before disposal to the environment [4,5]. Methylene blue (MB) is a basic dye and is the commonly used substance for dyeing cotton, wood, and silk [6]. MB can cause several harmful effects, such as increased heart rate, vomiting, shock, Heinz body formation, cyanosis, jaundice, quadriplegia, and tissue necrosis in humans [7]. Therefore, the removal of such a dye from process effluent becomes environmentally important.

Various treatment methods are available for the removal of dyes from wastewater. These methods include biotreatment [8–10], flocculation–coagulation [11], photocatalytic degradation [12], Fenton chemical oxidation [13,14], cation exchange membranes [15], and electrochemical degradation [16]. Adsorption is one of the most effective techniques of advance wastewater treatment and water re-use in terms of availability of different low-cost adsorbents. This technique provides high performance and convenience of operation and selectivity as well as exhibits a simple design and flexibility. Adsorption also does not result in the formation of harmful by-products [17]. Moreover, adsorption is an effective treatment method applicable for different categories of water pollutants, such as heavy metal [18,19], uncolored organic pollutants [20], and hazardous dyes [21–23].

The dye removal from wastewater by adsorption technique using commercially activated carbons is an effective treatment method. However, the high cost of this method has motivated the search for alternative industrial, agriculture, and biomass wastes as low-cost adsorbents. These alternatives include de-oiled soya [23], pineapple stem [24], oil palm trunk fiber [25], durian peel [26], guava leaf powder [27], almond shells [28], pomelo peel [29], broad bean peel [30], jackfruit peel [31], rice husk [32], palm kernel fiber [33], coconut bunch waste [34], grass waste [35], raw bagasse [36], banana leaves [37], papaya stem [38], platanus leaves [39], and lignite [40].

Malaysia weather benefits from a tropical climate with no winter, plenty of sunshine, rainfall, high temperatures, and high humidity throughout the year. Thus, this country has the highest rate of biomass production worldwide, generating large quantities of organic wastes, such as grass, leaves, and flowers [35]. In Malaysia, fallen coconut leaves (CLs) (*Cocos nucifera*) are one of the organic components of solid wastes without economic value and often cause serious disposal problems to the local environments.

This work aims to investigate the potential of fallen CLs, which are abundantly available solid wastes in Malaysia, as an adsorbent for the removal of MB from aqueous solutions. The influence of adsorption fundamental parameters, including adsorbent dose, initial dye concentration, pH, and contact time, on MB removal was investigated. A face-centered composite design (FCCD) by response surface methodology (RSM) was selected to elucidate the simultaneous effects of the fundamental parameters on the adsorption process. The multiple regression analysis technique was applied in the RSM to develop the equations and empirical models that correlate the MB removal efficiency to four adsorption variables. The analysis of variance (ANOVA) was also included to assess the adequacy of the model. The optimized conditions developed from the model were validated experimentally, and the CL feasibility for MB removal was also determined. Under optimal experimental conditions, the equilibrium isotherm and kinetics studies were performed. The RSM approach has been successfully applied to optimize the response efficiency and evaluate simple and combined effects of different variables on the response of several dye removal processes [12,36,41–48].

2. Materials and methods

2.1. Preparation of adsorbent/CL

Fallen CLs used as an adsorbent were collected from Universiti Teknologi MARA, Arau Campus, Perlis, Malaysia. The collected CLs were washed with water to remove all the dust and dissolvable substance. The leaves were then cut into small pieces (1–3 cm) and dried at 80˚C for 48 h using a hot air oven. The dried pieces were ground and sieved to obtain a particle size range of 150–212 μm of CL powder. Thirty grams of CL powder was washed with hot distilled water until the filtered water was clear. Subsequently, the CL powder was dried at 80˚C for 24 h in an oven and then stored in desiccators for further use. The CL powder was characterized using scanning electron microscopy (SEM; LeoSupra VP50; Carl-Zeiss, SMT, Germany) and Fourier transform infrared spectroscopy (FTIR; Nicolet, Thermo Electron Corporation).

2.2. Adsorbate/MB

MB a basic dye was purchased from R&M. MB with a molecular formula of $C_{16}H_{18}C1N_3S{\cdot}xH_2O$, a molecular weight of 319.86 g/mol, and a dye content of ~82% was chosen as adsorbate. The stock solution of MB was prepared (1,000 mg/L), and the desired concentration was obtained by diluting the stock solution with ultrapure water (18.2 MΩ/cm). The initial pH of the MB solution was adjusted with 0.1 mol/L HCl or 0.1 mol/L NaOH using a Metrohm 827 pH lab meter.

2.3. Experimental design

RSM is a technique used for developing an empirical model by mathematical and statistical analyses to optimize responses or output variables that are influenced by several input variables. RSM generates regression model equation and optimized conditions using a minimum number of experimental runs according to the experimental design [49–52].

A FCCD was applied for the present work. This rotatable design is suitable for fitting a quadratic surface and usually works well for process optimization [12]. To evaluate the influence of operating parameters on MB removal efficiency (response Y), we selected four independent variables, namely, adsorbent dosage (A), initial MB concentration (B), initial solution pH (C), and time agitation (D). For the four variables, 30 experiments were conducted including 16 experiments at factorial points, 8 experiments at axial points, and 6 replications at central points. All experiments were derived from Eq. (1) [53].

$$N = 2^n + 2n + n_c = 2^4 + 2(4) + 6 = 30 \quad (1)$$

where N is the total number of experiments required and n is the number of factors.

The variables (X_i) were coded as x_i according to Eq. (2) [48] to ease statistical calculations.

$$x_i = \frac{X_i - X_o}{\Delta X_i} \quad (2)$$

where X_o is the value of X_i at the center point, and ΔX_i presents the step with maximum and minimum values of variable X_i.

The correlation between response and independent variables associated with the central composite matrix was approximated by the following second-order quadratic polynomial equation [54]:

$$y = \beta_o + \sum_{i=1}^{k} \beta_i x_i + \sum_{i=1}^{k} \beta_{ii} x_i^2 + \sum_{i=1}^{k} \sum_{i \neq j=1}^{k} \beta_{ij} x_i x_j + \varepsilon \quad (3)$$

where y is the response (dependent variables) and β_0 is the constant coefficient. β_i, β_{ii}, and β_{ij} are linear, quadratic, and interaction coefficients, respectively, χ_i and χ_j are the coded values of variables, and ε is the residual term. Design-Expert software (version 7.0.0) (STAT-EASE Inc., Minneapolis, USA) was used for model-fitting steps, data analysis, and evaluation of the statistical significance of the equations.

2.4. Evaluation of the fitted model

The goodness of the fitted second-order polynomial model was evaluated by the coefficient of determination (R^2) and ANOVA.

2.5. Optimization analysis

Optimum conditions for variables including adsorbent dose (A), initial MB concentration (B), pH (C), and agitation time (D) were obtained using the data from statistical analysis. Design-Expert software was used to search for a combination of factors that simultaneously satisfy the requirements placed on each of the response and factor.

2.6. Batch experiments

MB removal experiments were conducted by varying the process parameters formed by FCCD. Based on the preliminary study, CL powder with a particle size of 150–212 μm was employed throughout the experiment. The range and level of variables that were used in this experimental design were 0.5–1.5 g/L for CL adsorbent dosages, 10–50 mg/L for initial MB concentration, 4–10 for initial pH of MB solution, and 5–45 min for contact times. For each run, 100 mL of the MB solution with certain concentration and initial pH was collected into a 250-mL Erlenmeyer flask. The adequately weighed adsorbent CL powder was added, and the flasks were agitated at room temperature (RT = 27 ± 2°C) using an orbital shaker (Model: SK 300; Lab-companion) at 120 rpm. After a certain duration, samples were collected, filtered using a nylon syringe filter (pore size of 0.2 μm, diameter of 25 mm; Whatman), and analyzed by a DR 2800 HACH spectrophotometer at a λ_{max} of 661 nm. The MB removal efficiency was calculated using the following equation:

$$\text{MB removal } (\%) = (C_i - C_f)/C_i \times 100 \quad (4)$$

where C_i is the initial MB concentration (mg/L) and C_f is the final MB concentration in solution (mg/L).

3. Results and discussion

3.1. Characterization of the prepared CL adsorbent

The surface morphology of CL-derived adsorbent powder was observed using the SEM technique. Fig. 1(a) and (b) shows the surface morphology of CL powder before MB adsorption at different magnifications. The CL material exhibited a rough surface and a porous structure. The surface condition of CL was responsible for its good adsorption property. After MB adsorption, the surface of the dye-loaded CLs displayed an irregular, non-porous, and compact structure because of the adsorbed MB dye molecules (Fig. 1(c)). FTIR analysis was performed to identify the main functional groups in CLs that may be involved in the adsorption process (spectra not shown). Table 1 shows the number of distinct absorption bands of CLs before and after MB adsorption. A number of absorption peaks were observed, indicating the complex nature of the prepared biomass. The results revealed sorbent heterogeneity, evidenced by the different characteristic peaks. The main functional groups that contributed to adsorption were –OH, C=O, C–O, C–H, and –COOH [55].

3.2. Statistical analysis

A batch study of the 30 experiments designed by Design-Expert software (runs) was performed to verify the effect of the four independent process variables including adsorbent dose (A), initial MB concentration (B), pH (C), and agitation time (D), and their interactive impacts on the MB removal efficiency (as response). A quadratic polynomial model was used to develop the mathematical relationship between the response and the independent process variables. The experimental and predicted results for MB removal efficiency at each point that were obtained for different combinations of selected variables are shown in Table 2.

3.3. Model validation

An ANOVA was carried out to assess the statistical significance of the FCCD model. The results of the second-order response surface model in the form of an ANOVA are shown in Table 3.

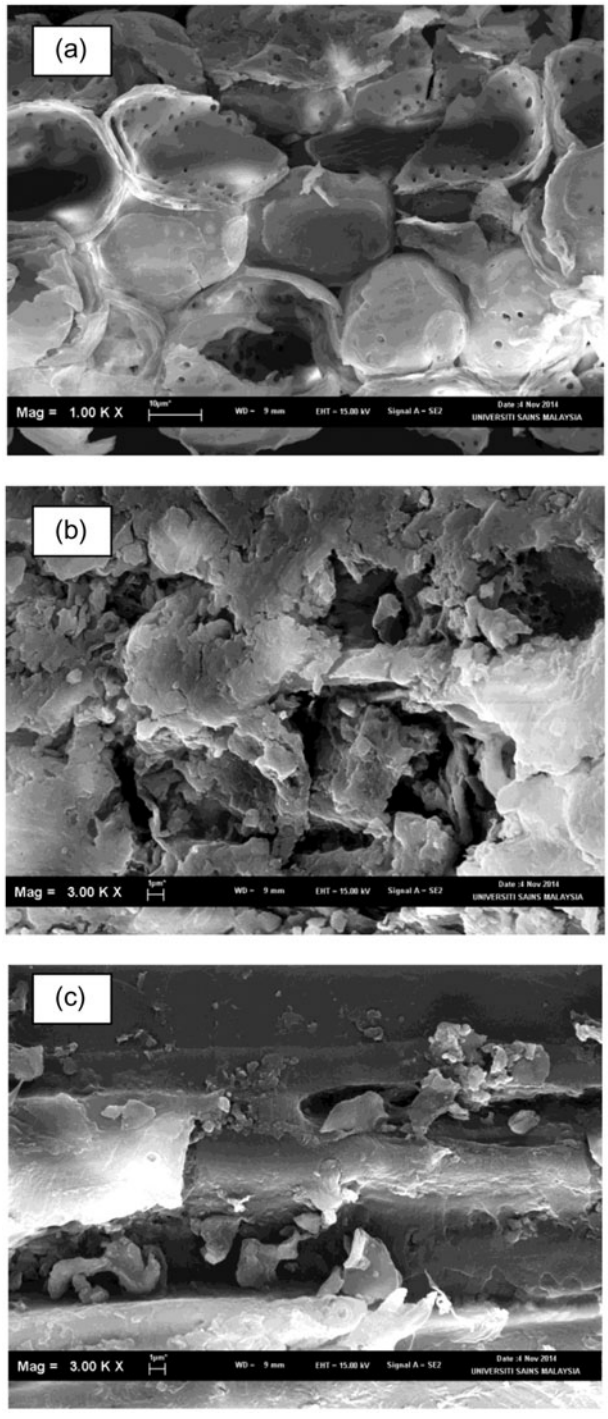

Fig. 1. SEM images of CL before adsorption at magnification 1.00 and 3.00 KX (a) and (b) respectively, image (c) for CL after MB adsorption at magnification 3.00 KX.

Values of model terms Prob > F < 0.0500 indicate that factors are significant under selected conditions. Significant model terms for response (MB removal %) were A, B, C, D, AC, AD, CD, A^2, B^2, C^2, and D^2.

Table 1
FT-IR spectral characteristics of CL before and after adsorption of MB

Wavelength range (cm^{-1})	Frequency (cm^{-1})		Difference	Assignment
	Before adsorption	After adsorption		
3,500–3,000	3,398.56	3,413.38	−14.82	Bonded—OH groups
2,900–2,800	2,920.57	2,921.23	−0.66	CH stretching
	2,855.16	2,853.40	1.76	
2,500–2,300	2,363.34	2,364.52	−1.18	O–H carboxylic acid
1,740–1,680	1,729.13	1,730.78	−1.65	C=O carbonyl group
1,620–1,680	1,608.99	1,639.56	−30.57	C=C stretching
1,500–1,400	1,448.29	1,449.52	−1.23	C–O stretching
1,080–1,360	1,238.02	1,244.28	−6.62	C–N stretching
1,070–1,150	1,052.09	1,062.20	−10.11	C–OH stretching

Table 2
FCCD for four independent variables with the observed response (MB removal %)

No. of runs	(A) Adsorbent dose (g/L)	(B) $[MB]_o$ (mg/L)	(C) pH	(D) Time (min)	MB removal %	
					Actual value	Predicted value
1	0.50	10.00	4.00	5.00	55.87	57.78
2	1.50	10.00	4.00	5.00	68.56	68.54
3	0.50	50.00	4.00	5.00	45.08	41.65
4	1.50	50.00	4.00	5.00	49.96	50.13
5	0.50	10.00	10.00	5.00	65.95	66.85
6	1.50	10.00	10.00	5.00	85.51	85.84
7	0.50	50.00	10.00	5.00	47.96	49.64
8	1.50	50.00	10.00	5.00	65.83	66.34
9	0.50	10.00	4.00	45.00	62.93	61.55
10	1.50	10.00	4.00	45.00	66.29	65.62
11	0.50	50.00	4.00	45.00	44.92	45.6
12	1.50	50.00	4.00	45.00	49.15	47.38
13	0.50	10.00	10.00	45.00	80.4	81.24
14	1.50	10.00	10.00	45.00	90.97	93.53
15	0.50	50.00	10.00	45.00	65.07	64.22
16	1.50	50.00	10.00	45.00	75.13	74.23
17	0.50	30.00	7.00	25.00	65.73	65.39
18	1.50	30.00	7.00	25.00	75.99	75.78
19	1.0	10.00	7.00	25.00	83.54	79.07
20	1.0	50.00	7.00	25.00	57.43	61.35
21	1.0	30.00	4.00	25.00	59.74	64.26
22	1.0	30.00	10.00	25.00	87.28	82.21
23	1.0	30.00	7.00	5.00	81.89	79.84
24	1.0	30.00	7.00	45.00	84.17	85.67
25	1.0	30.00	7.00	25.00	77.73	77.67
26	1.0	30.00	7.00	25.00	76.58	77.67
27	1.0	30.00	7.00	25.00	78.65	77.67
28	1.0	30.00	7.00	25.00	77.55	77.67
29	1.0	30.00	7.00	25.00	76.27	77.67
30	1.0	30.00	7.00	25.00	77.61	77.67

Table 3
ANOVA results for response surface quadratic model for MB removal

Source	Sum of squares	DF	Mean square	F value	Prob > F
Model	5,043.94	14	360.28	42.75	<0.0001
A	485.47	1	485.47	57.61	<0.0001
B	1,413.17	1	1,413.17	167.7	<0.0001
C	1,450.81	1	1,450.81	172.16	<0.0001
D	152.66	1	152.66	18.12	0.0007
A^2	130.25	1	130.25	15.46	0.0013
B^2	144.39	1	144.39	17.13	0.0009
C^2	51.08	1	51.08	6.06	0.0264
D^2	66.86	1	66.86	7.93	0.013
AB	5.22	1	5.22	0.62	0.4435
AC	67.65	1	67.65	8.03	0.0126
AD	44.82	1	44.82	5.32	0.0358
BC	1.16	1	1.16	0.14	0.7163
BD	0.034	1	0.034	4.06×10^{-3}	0.95
CD	112.89	1	112.89	13.4	0.0023
Residual	126.4	15	8.43		
Pure error	3.69	5	0.74		
Cor total	517.35	29			

The other remaining terms (AB, BC, and BD) had less significance for the response and could be neglected to improve the model. Thus, the equation developed is expressed as follows:

$$\text{MB removal } \% = +77.67 + 5.19A - 8.86B + 8.98C + 2.91D + 2.06AC - 1.67AD + 2.66CD - 7.09A^2 - 7.47B^2 - 4.44C^2 + 5.08D^2 \quad (5)$$

The goodness of fit of the model was also tested by the multiple correlation coefficients (R^2). In this case, the value of the multiple correlation coefficients was 0.9756. This value implies that the regression is statistically significant, and only 2.44% of the total variations is unexplained by the model. This result can be observed in Fig. 2 by comparing the actual values against the predicted responses by the model for the percentage of MB removal. The value of the predicted multiple correlation coefficient (pred. $R^2 = 0.8778$) agrees well with the value of the adjusted multiple correlation coefficient (adj. $R^2 = 0.9527$).

The analysis of the residuals (difference between the observed and the predicted response values) provides useful information about model suitability. This analysis identifies the outliers and examines the diagnostic plots, such as normal probability and residual plots. The normal probability plots show whether the residuals follow a normal distribution, in which case the points will follow a straight line [56]. The plot of normal probability of the residual for MB removal is depicted in Fig. 3. The trend reveals a reasonably well-behaved residual of the MB dye, and the residual is normally distributed and resembles a straight line. Moreover, residual vs. predicted response was plotted and is shown in Fig. 4. The plot shows the residual vs. the ascending predicted response value, which tests the assumption of constant variance. The points in the plot are randomly scattered with a constant range of

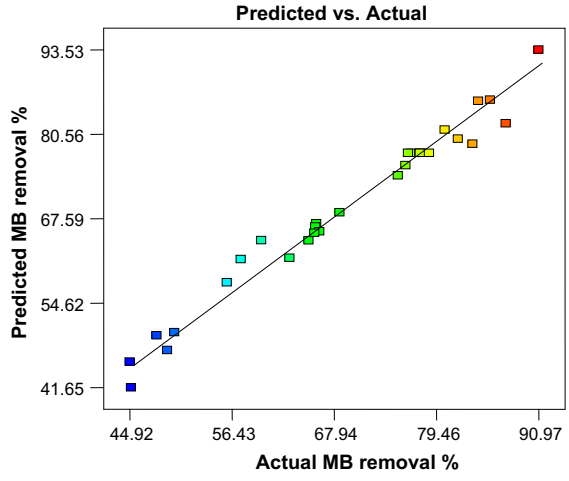

Fig. 2. Comparison of the actual results of MB removal % with the predicted values by FCCD model.

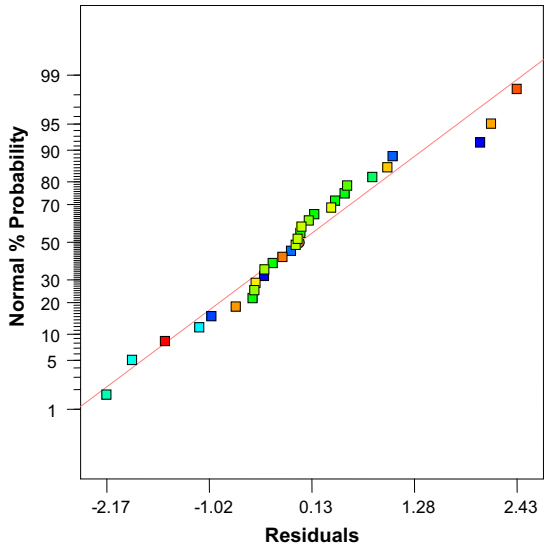

Fig. 3. Normal probability plots for MB removal efficiency.

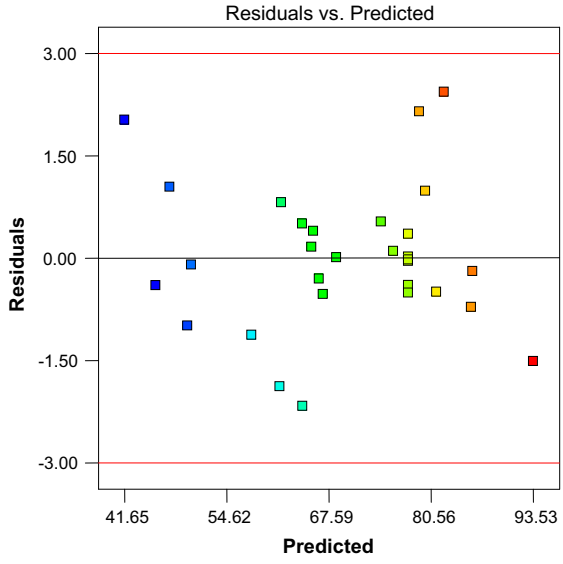

Fig. 4. Residual vs. predicted response values for MB removal efficiency.

residuals across the graph. Fig. 4 demonstrates that the residuals in the plot fluctuate in a random pattern around the center line.

3.4. Effect of independent variables

Perturbation plots were used to investigate the individual effect of the four independent variables, including adsorbent dose (factor A), initial MB concentration (factor B), pH (factor C), and time of agitation (factor D), on the MB removal. A perturbation plot employs the model terms to show the influence of each factor deviation from the reference point on the process response, while holding the other factors constant. Design-Expert software automatically sets the reference point at the midpoint (coded 0) of all the factors. The perturbation plot can be applied to investigate the most significant factors on the response. A steep slope or curvature in a factor shows that the response is sensitive to that variable. A relatively flat line indicates response insensitivity to change in that particular variable [57]. Perturbation plots for the MB removal efficiency are shown in Fig. 5. A sharp curvature for all the independent variables suggests that the response of the MB removal efficiency was very sensitive to all the parameters. In general, the MB removal efficiency increased with increasing time of agitation (factor C), adsorbent dose (factor A), and pH (factor B). Meanwhile, the MB removal efficiency increased as the initial MB concentration decreased.

3.5. Interaction effects on responses and process optimization

ANOVA results for the response parameter (Table 3) indicated that maximum MB removal (%) can be obtained under the following interaction terms: AC, AD, and CD. Figs. 6–8 show the 3D and contour plots of the response at the optimal interaction terms of AC, AD, and CD, respectively, and simultaneously

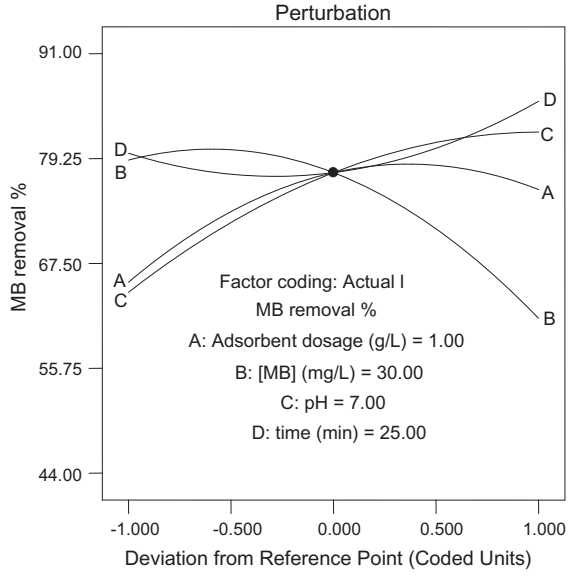

Fig. 5. Perturbation plots for MB removal efficiency. (A) Adsorbent dose (g/L); (B) $[MB]_o$ (mg/L); (C) pH; (D) agitation time (min).

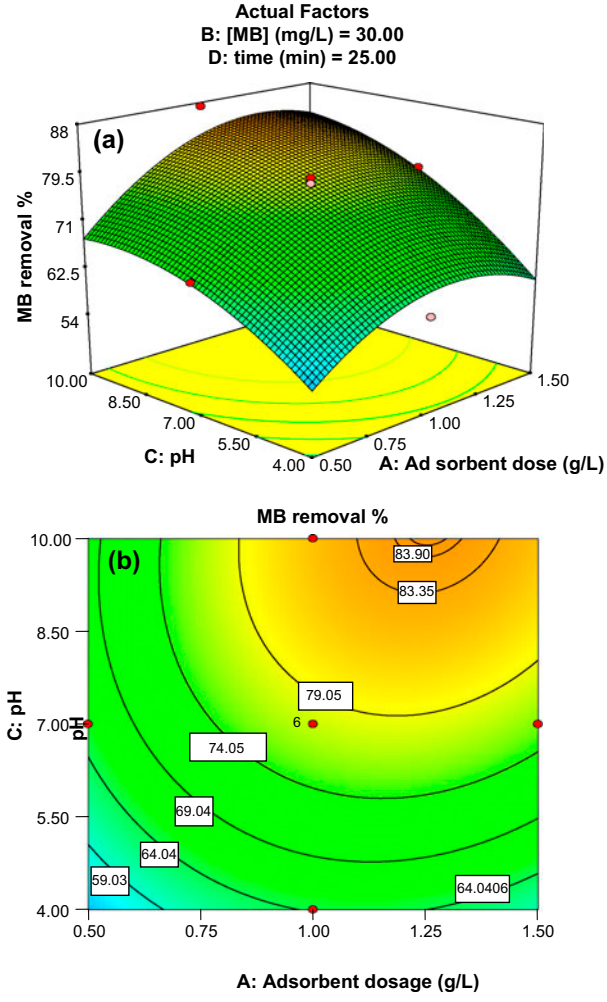

Fig. 6. 3-D response surface (a) and contour plots (b) of the MB removal efficiency as the function of adsorbent dose and pH ($[MB]_o$ = 30.00 mg/L and agitation time = 25.00 min).

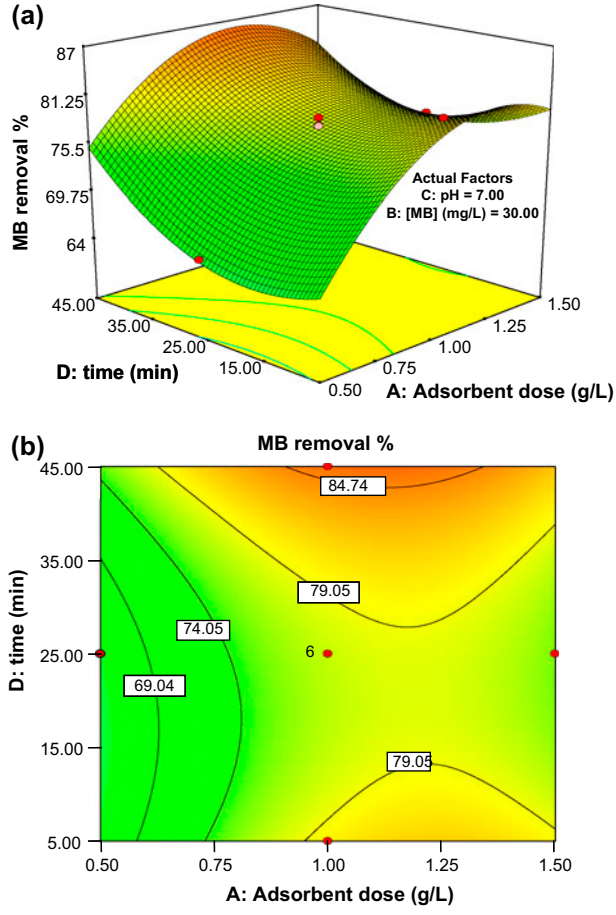

Fig. 7. 3-D response surface (a) and contour plots (b) of the MB removal efficiency as the function of adsorbent dose and agitation time ($[MB]_o$ = 30.00 mg/L and pH 7.00).

keeping the other two variables constant at the central level.

The combined effect of adsorbent dose (A) and pH (C) on MB removal efficiency (response) was significant (p = 0.0126, Table 3), and the MB removal efficiency at 30 mg/L dye concentration and 25-min agitation time is shown in the 3D and contour plots of Fig. 6(a) and (b), respectively. Adsorbent dose reveals the ability of the CL adsorbent to uptake MB molecules from a given solution. Meanwhile, the initial solution pH is responsible for the surface charge. Hence, the interaction effect influences the model. The MB removal efficiency increased to 83.90% with a simultaneous increase in adsorbent dose and basic solution pH. The optimum CL dose was approximately 1.25 g/L as the adsorption process reached equilibrium with this dosage and remained stable with increasing CL masses. In general, increasing the adsorbent dose provides a greater surface area and increases the availability of the binding sites [58]. The low MB removal at acidic solution pH can be attributed to the availability of H_3O^+ ions that compete with the dye cations for the adsorption sites. This is also a favorable characteristic of an adsorbent for real wastewater decolorization from textile industry that is alkaline in nature to avoid additional costs caused by pH control [59]. A similar behavior was observed for MB removal using different types of biomass adsorbent [24,25,31,39].

The combined effect of adsorbent dose (A) and agitation time (D) on MB removal efficiency (response) was significant (p = 0.0358, Table 3). The MB removal efficiency at 30 mg/L dye concentration and initial pH 7 is shown in the 3D and contour plots of Fig. 7(a) and (b), respectively. Time of agitation offers better contact between the dye and CL particles. The MB

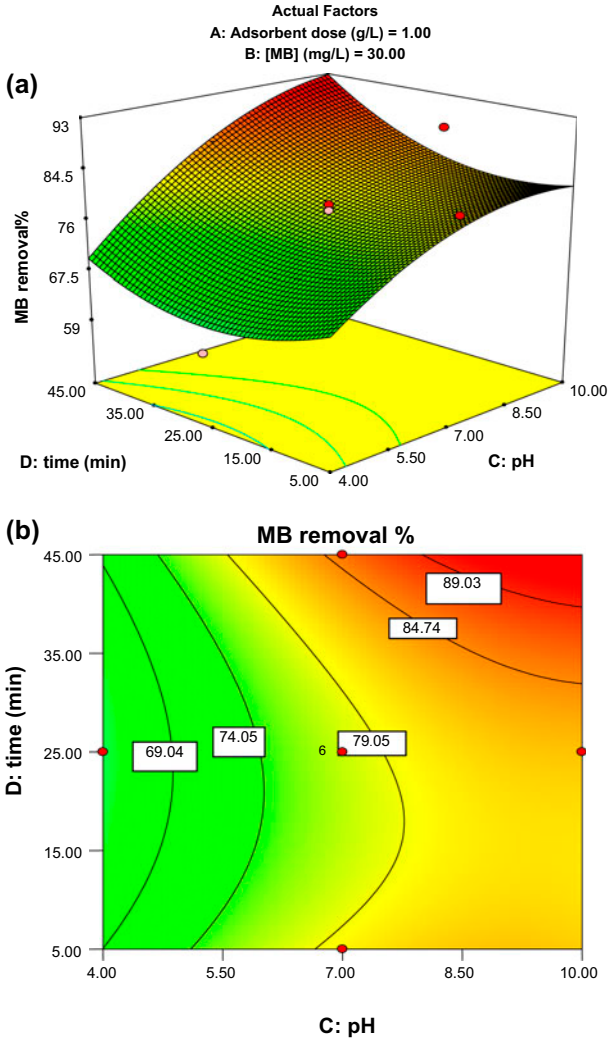

Fig. 8. 3-D response surface (a) and contour plots (b) of the MB removal efficiency as the function of pH and agitation time (adsorbent dose = 1.00 g/L and $[MB]_o$ = 30.00 mg/L and pH 7.00).

removal efficiency increased to 84.74% by simultaneously increasing agitation time and CL dose. However, no remarkable change was observed in MB removal after reaching 1.25 g/L CL adsorbent dose even with longer agitation times. This result may be attributed to the aggregation of CL particles at high doses [60], which leads to a screening effect [61]. Such aggregation results in a decrease in the total surface area of the adsorbent, decreasing dye removal efficiency [62].

The combined effect of initial pH (C) and agitation time (D) on MB removal efficiency (response) was significant (p = 0.0023, Table 3), and the MB removal efficiency at 30 mg/L dye concentration and 1.0 g/L CL dose is shown in the 3D and contour plots of Fig. 8. MB removal efficiency rapidly increased to 89.03% with a simultaneous increase in agitation time and initial pH. Longer agitation times allow the MB molecules more chances to penetrate into the interior surface of CL adsorbent pore after the adsorption sites available on the exterior surface of the CL particles are occupied during the first period of agitation time.

3.6. Confirmation experiment

We confirmed the optimized data given using numerical modeling under optimized conditions. The optimum predicted conditions identified were adsorbent dosage of 1.26 g/L, initial MB concentration of 19.01 mg/L, pH of 8.65, and contact time of 5.00 min. The MB removal efficiency (response) of the experimental optimal conditions was 86.38%, whereas that of the predicted response was 87.09% under the same conditions. This observation indicates that the deviation of predicted % removal and actual % removal was less. Given these optimal results, pH of 8.65 and CL powder dosage of 1.26 g/L were chosen for all the following studies.

3.7. Effect of initial MB dye concentration

The equilibrium contact time is crucial for determining the adsorption capacity of the adsorbents. The adsorbed amount of MB at time t, q_t (mg/g), was calculated as follows:

$$q_t = \frac{(C_0 - C_t)V}{W} \tag{6}$$

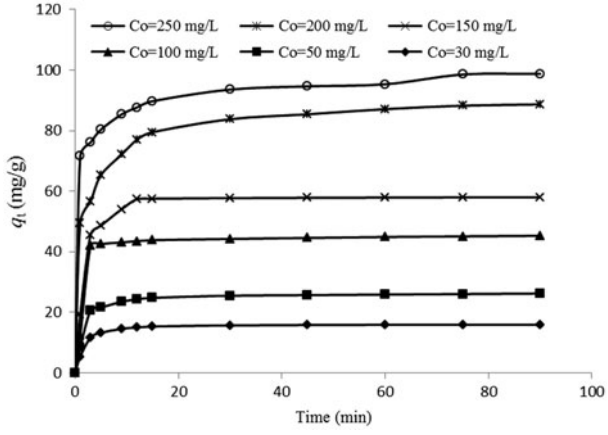

Fig. 9. Effect of initial dye concentration and contact time on the adsorption capacity of MB onto CL surface [CL dose = 0.252 g, V: 200 mL; pH 8.65; and T: 27 ± 2°C].

where C_t (mg/L) is the liquid-phase concentration of MB solution at time t (min). Fig. 9 shows the effect of contact time on the adsorption capacity of CLs for MB at different initial MB concentrations. The adsorption capacities of the MB dye on CLs increased with increasing initial concentrations and time. At very low initial MB concentrations, the adsorbent rapidly reached equilibrium. However, when the concentration increased from 150 to 250 mg/L, the adsorptive uptake of the MB dye also increased and took longer to reach equilibrium. A high uptake at higher initial concentrations may occur because of the formation of driving force by the mass gradient between solutions and the adsorbent that leads to high amounts of MB molecules being transferred to the CL surface. A similar result was described by Kong et al. [39] for the uptake of MB on the surface of Platanus leaves.

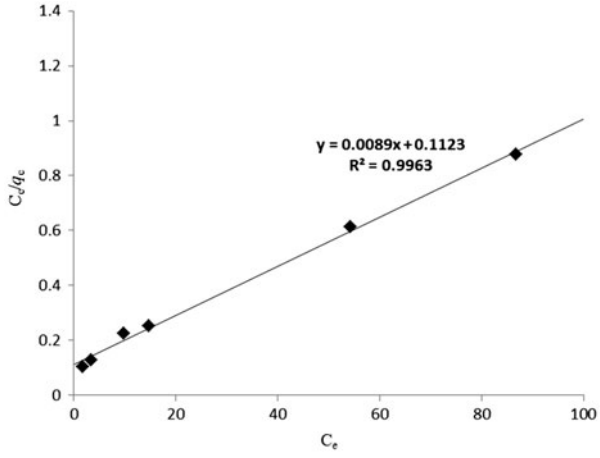

Fig. 10. Langmuir isotherm plots for MB dye adsorption onto CL.

3.8. Adsorption isotherm studies

Adsorption isotherm reveals the relationship between the mass of adsorbate adsorbed per unit weight of adsorbent in equilibrium and liquid-phase equilibrium concentration of the adsorbate [63]. To quantify the adsorption capacity of CLs for the removal of the MB dye from aqueous solutions, we tested the Langmuir, Freundlich, and Temkin isotherm models.

3.8.1. Langmuir model

The Langmuir model assumes that adsorptions occur at specific homogeneous sites on the adsorbent. This model is successfully used in numerous monolayer adsorption processes [64]. The data of the equilibrium studies for the adsorption of the MB dye onto CLs may follow the Langmuir model as follows:

$$\frac{C_e}{q_e} = \frac{1}{q_m K_L} + \frac{1}{q_m} C_e \tag{7}$$

where C_e is the equilibrium concentration (mg/L) and q_e is the amount adsorbed per specified amount of adsorbent (mg/g), K_L is the Langmuir equilibrium constant, and q_m is the amount of adsorbate required to form a monolayer. Hence, a plot of C_e/q_e vs. C_e should be a straight line with a slope $(1/q_m)$ and an intercept $(1/q_m K_L)$ (Fig. 10). The Langmuir-type adsorption isotherm indicates the surface homogeneity of the adsorbent. The adsorbent surface is made up of small adsorption patches, which are energetically equivalent to each other in terms of adsorption phenomenon. The correlation coefficient (R^2) value of 0.9963 revealed that the adsorption data of the MB dye onto CLs fitted well with the Langmuir isotherm. The values of constants K_L and b were calculated and the results are shown in Table 4.

The essential characteristics of the Langmuir isotherm can be expressed in terms of separation factor R_L, a dimensionless constant [65], which is given by:

$$R_L = \frac{1}{(1 + K_L C_0)} \tag{8}$$

An adsorption system is considered favorable when $0 < R_L < 1$, unfavorable when $R_L > 1$, linear when $R_L = 1$, or irreversible when $R_L = 0$. In this study, the values of R_L obtained were between 0 and 1. Therefore, the adsorption process is favorable. The calculated R_L values at different initial MB

Table 4
Isotherm parameters for MB adsorption on CL at 27 ± 2°C

Isotherm	Parameter	Value
Langmuir	q_m (mg/g)	112.35
	K_L (L/mg)	0.0792
	R^2	0.9963
Freundlich	K_F ((mg/g) (L/mg)$^{1/n}$)	14.42
	n	2.18
	R^2	0.9749
Temkin	K_T (L/mg)	1.0301
	B	21.613
	R^2	0.9879

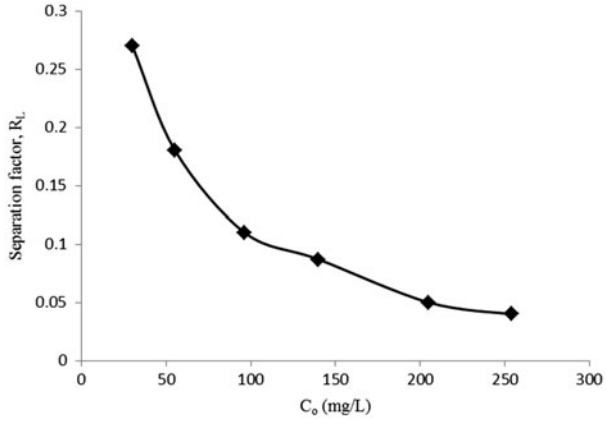

Fig. 11. Values of the separation factor, R_L, for the adsorption of the MB dye onto CL at different initial MB concentrations.

concentrations are shown in Fig. 11. The R_L value, which was within the range of 0–1 at all initial dye concentrations, confirms the favorable uptake of MB over the entire range of concentration levels.

3.8.2. Freundlich model

The Freundlich model can be applied for non-ideal adsorption on heterogeneous surfaces and multilayer adsorption [66]. This model is presented as follows:

$$q_e = (K_F)\left(C_e^{\frac{1}{n}}\right) \tag{9}$$

$$\ln q_e = \ln K_F + \frac{1}{n}\ln C_e \tag{10}$$

where K_F is the Freundlich equilibrium constant, n is an empirical constant, and the rest of the terms have the usual significance. Thus, a plot of $\ln q_e$ vs. $\ln C_e$ should be a straight line with a slope $1/n$ and an intercept of $\ln K_F$ (Fig. 12). The related parameters were calculated, and the results are shown in Table 4.

3.8.3. Temkin model

Temkin and Pyzhev [67] considered the effects of indirect adsorbate/adsorbate interactions on adsorption isotherms. The Temkin isotherm was used in the following form:

$$q_e = \left(\frac{RT}{b}\right)\ln(K_T C_e) \tag{11}$$

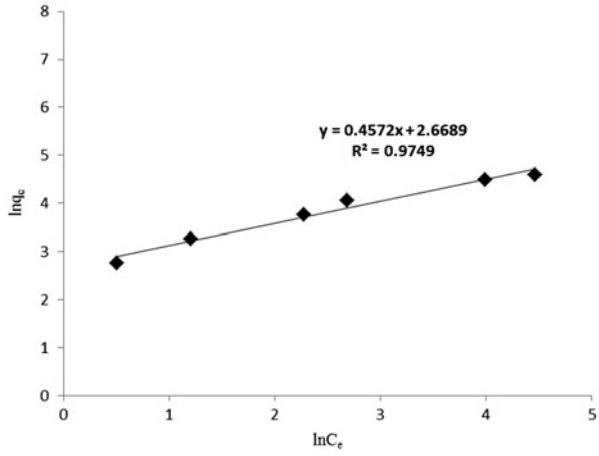

Fig. 12. Freundlich isotherm plots for MB dye adsorption onto CL.

This equation can be expressed in its linear form as follows:

$$q_e = B\ln K_T + B\ln C_e \tag{12}$$

where $B = (RT/b)$, a plot of q_e vs. $\ln C_e$ yielded a linear line (Fig. 13), enables to determine the isotherm constants K_T and B. K_T is the Temkin equilibrium binding constant (L/mg) that corresponds to the maximum binding energy, and constant B is related to adsorption heat. The adsorption heat of all the molecules in the layer is expected to decrease linearly with coverage because of adsorbate/adsorbate interactions. The constants K_T and B as well as the R^2 values are shown in Table 4. The Langmuir model fitted the data better than the Freundlich and Temkin models (Table 4).

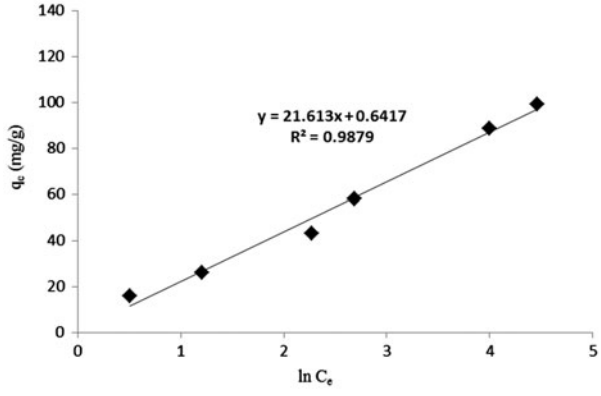

Fig. 13. Temkin isotherm plots for MB dye adsorption onto CL.

Table 5
Comparison of the adsorption capacity for MB by various adsorbents reported in the literature

Adsorbent	q_m (mg/g)	Ref.
Pineapple stem	119.05	[24]
Guava leaf	295.00	[27]
Broad bean peels	192.70	[30]
Coconut bunch waste	70.92	[34]
Platanus leaf	145.62	[39]
Untreated lignite	41.94	[40]
Cogongrass	27.40	[68]
Orange peel	18.60	[69]
Wheat shells	16.56	[70]
Coconut leaf	112.35	This work

This result is also confirmed by the high R^2 value for the Langmuir model (0.9963) compared with the Temkin (0.9879) and Freundlich (0.9749) models. Therefore, the adsorption of MB on CLs occurs as monolayer adsorption on a surface that is homogenous in adsorption affinity. The computed maximum monolayer adsorption capacity (q_m) of CLs for MB was 112.35 mg/g (Table 4). The maximum sorption capacity (q_m) of the CL adsorbent for MB was compared with those reported in the literature for different adsorbents/MB adsorption systems (Table 5).

3.9. Kinetic studies

The pseudo-first-order model and pseudo-second-order model were used to investigate the adsorption kinetics of the MB dye on CLs. The conformity between experimental data and the model predicted values was expressed by correlation coefficient (R^2).

3.9.1. Pseudo-first-order model

The pseudo-first order rate model of Lagergren [71] is based on solid capacity and generally expressed as follows:

$$\ln(q_e - q) = \ln(q_e) - (k_1)t \tag{13}$$

where q_e is the amount of solute adsorbed at equilibrium per unit weight of adsorbent (mg/g), q is the amount of solute adsorbed at any time (mg/g), and k_1 is the adsorption constant. This expression is the most popular form of the pseudo-first-order kinetic model. k_1 values at different initial MB concentrations were calculated from the plots of $\ln(q_e - q)$ vs. t. Constant k_1 and correlation coefficients (R^2) were calculated and summarized (Table 6). The correlation coefficient (R^2) values obtained were relatively low; hence, this model has very poor correlation coefficients (R^2) for the best fit data.

3.9.2. Pseudo-second-order model

The kinetic data were analyzed using the pseudo-second-order model [72], which can be expressed as follows:

$$\frac{t}{q} = \left(\frac{1}{k_2 q_e^2}\right) + \left(\frac{1}{q_e}\right)t \tag{14}$$

The plot of t/q vs. t should give a linear relationship, from which q_e and k_2 can be determined from the slope and intercept of the plot. The k_2 and q_e determined from the model along with the

Table 6
Pseudo-first-order and pseudo-second-order kinetic parameters values at different initial concentrations with R^2 and for MB adsorption on CL

	C_o (mg/L)					
Parameters	30	50	100	150	200	250
$q_{e,\ exp.}$ (mg/g)	15.88	26.19	45.26	57.97	88.67	98.76
Pseudo-first-order						
$q_{e\ cal.}$(mg/g)	6.18	7.26	4.98	7.48	29.85	24.88
k_1 (1/m)	0.1125	0.0558	0.0457	0.0818	0.0544	0.0506
R^2	0.8993	0.8207	0.7278	0.7991	0.9676	0.8623
Pseudo-second-order						
$q_{e\ cal.}$ (mg/g)	16.0771	26.5251	45.662	58.82	90.09	99.00
k_2 (g/mg min)	0.0655	0.0292	0.0242	0.0196	0.0059	0.0074
R^2	0.9998	0.9999	0.9996	0.9998	0.9998	0.9995

corresponding correlation coefficient (R^2) values are presented in Table 6. The values of the calculated and experimental q_e are also presented in Table 6. Based on the given data, the adsorption of the MB dye perfectly followed the pseudo-second-order kinetic model.

4. Conclusion

In this work, the feasibility of MB adsorption onto fallen CLs as agricultural wastes that are largely available in Malaysia was investigated. RSM and FCCD were suitable in determining the optimal conditions for adsorption, including adsorbent dose, initial MB concentration, pH, and agitation time. Results indicated that fallen CLs can be used to remove lead basic dye (MB) from aqueous solution. The amount of MB dye uptake (mg/g) increased with increasing contact time, pH, and initial dye concentration. The equilibrium data fit very well with the Langmuir isotherm equation, confirming the monolayer adsorption capacity of the MB dye onto CLs with a monolayer adsorption capacity of 112.35 mg/g at 27 ± 2˚C. The rate of adsorption followed a pseudo-second-order kinetics with a good correlation. These results demonstrate that fallen CLs are economically feasible for the removal of basic dye from aqueous solutions.

Acknowledgments

The authors would like to thank the Ministry of Education, Malaysia for funding this research work under the Research Acculturation Grant Scheme (600-RMI/RAGS 5/3(18/2014). The authors also thank the Research Management Institute (RMI) and the Universiti Teknologi MARA for supporting the research work.

References

[1] R.O.A. deLima, A.P. Bazo, D.M.F. Salvadori, C.M. Rech, D.P. Oliveira, G.A. Umbuzeiro, Mutagenic and carcinogenic potential of a textile azo dye processing plant effluent that impacts a drinking water source, Mutat. Res. 626 (2007) 53–60.

[2] M.S. Tsuboy, J.P.F. Angeli, M.S. Mantovani, S. Knasmüller, G.A. Umbuzeiro, L.R. Ribeiro, Genotoxic, mutagenic and cytotoxic effects of the commercial dye CI Disperse Blue 291 in the human hepatic cell line HepG2, Toxicol. In Vitro 21 (2007) 1650–1655.

[3] R. Caritá, M.A. Marin-Morales, Induction of chromosome aberrations in the *Allium cepa* test system caused by the exposure of seeds to industrial effluents contaminated with azo dyes, Chemosphere 72 (2008) 722–725.

[4] F.A. Pavan, S.L.P. Dias, E.C. Lima, E.V. Benvenutti, Removal of Congo red from aqueous solution by anilinepropylsilica xerogel, Dyes Pigm. 76 (2008) 64–69.

[5] F.A. Pavan, Y. Gushikem, A.S. Mazzocato, S.L.P. Dias, E.C. Lima, Statistical design of experiments as a tool for optimizing the batch conditions to methylene blue biosorption on yellow passion fruit and mandarin peels, Dyes Pigm. 72 (2007) 256–266.

[6] B.H. Hameed, A.L. Ahmad, K.N.A. Latiff, Adsorption of basic dye (methylene blue) onto activated carbon prepared from rattan sawdust, Dyes Pigm. 75 (2007) 143–149.

[7] P.S. Kumar, S. Ramalingam, K. Sathishkumar, Removal of methylene blue dye from aqueous solution by activated carbon prepared from cashew nut shell as a new low-cost adsorbent, Korean J. Chem. Eng. 28 (2011) 149–155.

[8] M.M. El-Sheekh, M.M. Gharieb, G.W. Abou-El-Souod, Biodegradation of dyes by some green algae and cyanobacteria, Int. Biodeterior. Biodegrad. 63 (2009) 699–704.

[9] A.R. Khataee, A. Movafeghi, S. Torbati, S.Y. Salehi Lisar, M. Zarei, Phytoremediation potential of duckweed (*Lemna minor* L.) in degradation of C.I. Acid Blue 92: Artificial neural network modeling, Ecotoxicol. Environ. Saf. 80 (2012) 291–298.

[10] A.R. Khataee, G. Dehghan, M. Zarei, E. Ebadi, M. Pourhassan, Neural network modeling of biotreatment of triphenylmethane dye solution by a green macroalgae, Chem. Eng. Res. Des. 89 (2011) 172–178.

[11] P. Cañizares, F. Martínez, C. Jiménez, J. Lobato, M.A. Rodrigo, Coagulation and electrocoagulation of wastes polluted with dyes, Environ. Sci. Technol. 40 (2006) 6418–6424.

[12] A.H. Jawad, A.F.M. Alkarkhi, N.S.A. Mubarak, Photocatalytic decolorization of methylene blue by an immobilized TiO_2 film under visible light irradiation: Optimization using response surface methodology (RSM), Desalin. Water Treat. (2014) 1–12, doi: 10.1080/19443994.2014.934736.

[13] Y.S. Woo, M. Rafatullah, A.F.M. Al-Karkhi, T.T. Tow, Removal of Terasil Red R dye by using Fenton oxidation: A statistical analysis, Desalin. Water Treat. 53 (2013) 1–9.

[14] A.R. Khataee, M. Safarpour, A. Naseri, M. Zarei, Photoelectro-Fenton/nanophotocatalysis decolorization of three textile dyes mixture: Response surface modeling and multivariate calibration procedure for simultaneous determination, J. Electroanal. Chem. 672 (2012) 53–62.

[15] J.S. Wu, C.H. Liu, K.H. Chu, S.Y. Suen, Removal of cationic dye methyl violet 2B from water by cation exchange membranes, J. Membr. Sci. 309 (2008) 239–245.

[16] L. Fan, Y. Zhou, W. Yang, G. Chen, F. Yang, Electrochemical degradation of aqueous solution of Amaranth azo dye on ACF under potentiostatic model, Dyes Pigm. 76 (2008) 440–446.

[17] M. Rafatullah, O. Sulaiman, R. Hashim, A. Ahmad, Adsorption of methylene blue on low-cost adsorbents: A review, J. Hazard. Mater. 177 (2010) 70–80.

[18] H. Daraei, A. Mittal, J. Mittal, H. Kamali, Optimization of Cr(VI) removal onto biosorbent eggshell

membrane: Experimental & theoretical approaches, Desalin. Water Treat. 52 (2014) 1307–1315.
[19] H. Daraei, A. Mittal, M. Noorisepehr, J. Mittal, Separation of chromium from water samples using eggshell powder as a low-cost sorbent: Kinetic and thermodynamic studies, Desalin. Water Treat. 53 (2015) 214–220.
[20] H. Daraei, A. Mittal, M. Noorisepehr, F. Daraei, Kinetic and equilibrium studies of adsorptive removal of phenol onto eggshell waste, Environ. Sci. Pollut. Res. 20 (2013) 4603–4611.
[21] A. Mittal, V. Thakur, J. Mittal, H. Vardhan, Process development for the removal of hazardous anionic azo dye Congo red from wastewater by using hen feather as potential adsorbent, Desalin. Water Treat. 52 (2014) 227–237.
[22] J. Mittal, V. Thakur, A. Mittal, Batch removal of hazardous azo dye Bismark Brown R using waste material hen feather, Ecol. Eng. 60 (2013) 249–253.
[23] A. Mittal, J. Mittal, L. Kurup, A.K. Singh, Process development for the removal and recovery of hazardous dye erythrosine from wastewater by waste materials-bottom ash and de-oiled soya as adsorbents, J. Hazard. Mater. 138 (2006) 95–105.
[24] B.H. Hameed, R.R. Krishni, S.A. Sata, A novel agricultural waste adsorbent for the removal of cationic dye from aqueous solutions, J. Hazard. Mater. 162 (2009) 305–311.
[25] B.H. Hameed, M.I. El-Khaiary, Batch removal of malachite green from aqueous solutions by adsorption on oil palm trunk fibre: Equilibrium isotherms and kinetic studies, J. Hazard. Mater. 154 (2008) 237–244.
[26] B.H. Hameed, H. Hakimi, Utilization of durian (*Durio zibethinus Murray*) peel as low cost sorbent for the removal of acid dye from aqueous solutions, Biochem. Eng. J. 39 (2008) 338–343.
[27] V. Ponnusami, S. Vikram, S.N. Srivastava, Guava (*Psidium guajava*) leaf powder: Novel adsorbent for removal of methylene blue from aqueous solutions, J. Hazard. Mater. 152 (2008) 276–286.
[28] F.D. Ardejani, K. Badii, N.Y. Limaee, S.Z. Shafaei, A.R. Mirhabibi, Adsorption of direct red 80 dye from aqueous solution onto almond shells: Effect of pH, initial concentration and shell type, J. Hazard. Mater. 151 (2008) 730–737.
[29] B.H. Hameed, D.K. Mahmoud, A.L. Ahmad, Sorption of basic dye from aqueous solution by pomelo (*Citrus grandis*) peel in a batch system, Colloids Surf., A 316 (2008) 78–84.
[30] B.H. Hameed, M.I. El-Khaiary, Sorption kinetics and isotherm studies of a cationic dye using agricultural waste: Broad bean peels, J. Hazard. Mater. 154 (2008) 639–648.
[31] B.H. Hameed, Removal of cationic dye from aqueous solution using jackfruit peel as non-conventional low-cost adsorbent, J. Hazard. Mater. 162 (2009) 344–350.
[32] R. Han, D. Ding, Y. Xu, W. Zou, Y. Wang, Y. Li, L. Zou, Use of rice husk for the adsorption of congo red from aqueous solution in column mode, Bioresour. Technol. 99 (2008) 2938–2946.
[33] A.E. Ofomaja, Y.S. Ho, Equilibrium sorption of anionic dye from aqueous solution by palm kernel fibre as sorbent, Dyes Pigm. 74 (2007) 60–66.
[34] B.H. Hameed, D.K. Mahmoud, A.L. Ahmad, Equilibrium modeling and kinetic studies on the adsorption of basic dye by a low-cost adsorbent: Coconut (*Cocos nucifera*) bunch waste, J. Hazard. Mater. 158 (2008) 65–72.
[35] B.H. Hameed, Grass waste: A novel sorbent for the removal of basic dye from aqueous solution, J. Hazard. Mater. 166 (2009) 233–238.
[36] L.W. Low, T.T. Teng, A.F.M. Alkarkhi, A. Ahmad, N. Morad, Optimization of the adsorption conditions for the decolorization and COD reduction of methylene blue aqueous solution using low-cost adsorbent, Water Air Soil Pollut. 214 (2011) 185–195.
[37] R.R. Krishni, K.Y. Foo, B.H. Hameed, Adsorptive removal of methylene blue using the natural adsorbent-banana leaves, Desalin. Water Treat. 53 (2013) 1–9.
[38] R.R. Krishni, K.Y. Foo, B.H. Hameed, Adsorption of cationic dye using a low-cost biowaste adsorbent: Equilibrium, kinetic, and thermodynamic study, Desalin. Water Treat. 53 (2013) 1–8.
[39] L. Kong, L. Gong, J. Wang, Removal of methylene blue from wastewater using fallen leaves as an adsorbent, Desalin. Water Treat. 53 (2015) 2489–2500.
[40] A. Gürses, A. Hassani, M. Kıranşan, Ö. Açışlı, S. Karaca, Removal of methylene blue from aqueous solution using by untreated lignite as potential low-cost adsorbent: Kinetic, thermodynamic and equilibrium approach, J. Water Process Eng. 2 (2014) 10–21.
[41] M.B. Kasiri, A.R. Khataee, Removal of organic dyes by UV/H_2O_2 process: Modeling and optimization, Environ. Technol. 33 (2011) 1417–1425.
[42] M. Rastegar, K.R. Shadbad, A.R. Khataee, R. Pourrajab, Optimization of photocatalytic degradation of sulphonated diazo dye C.I. reactive green 19 using ceramic-coated TiO_2 nanoparticles, Environ. Technol. 33 (2011) 995–1003.
[43] A.R. Khataee, M. Zarei, L. Moradkhannejhad, S. Nourie, B. Vahid, Nitrogen doping of commercial TiO_2 nanoparticles for enhanced photocatalytic degradation of dye under visible light: Central composite design approach, Adv. Chem. Lett. 1 (2013) 24–31.
[44] K. Ravikumar, S. Krishnan, S. Ramalingam, K. Balu, Optimization of process variables by the application of response surface methodology for dye removal using a novel adsorbent, Dyes Pigm. 72 (2007) 66–74.
[45] B.H. Hameed, I.A.W. Tan, A.L. Ahmad, Optimization of basic dye removal by oil palm fibre-based activated carbon using response surface methodology, J. Hazard. Mater. 158 (2008) 324–332.
[46] K. Ravikumar, S. Ramalingam, S. Krishnan, K. Balu, Application of response surface methodology to optimize the process variables for reactive red and acid brown dye removal using a novel adsorbent, Dyes Pigm. 70 (2006) 18–26.
[47] M.K. Satapathy, P. Das, Optimization of crystal violet dye removal using novel soil-silver nanocomposite as nanoadsorbent using response surface methodology, J. Environ. Chem. Eng. 2 (2014) 708–714.
[48] A. Hassani, L. Alidokht, A.R. Khataee, S. Karaca, Optimization of comparative removal of two structurally different basic dyes using coal as a low-cost and available adsorbent, J. Taiwan Inst. Chem. Eng. 45 (2014) 1597–1607.

[49] A. Baçaoui, A. Yaacoubi, A. Dahbi, C. Bennouna, R.P.T. Phan Tan Luu, F.J. Maldonado-Hodar, J. Rivera-Utrilla, C. Moreno-Castilla, Optimization of conditions for the preparation of activated carbons from olive-waste cakes, Carbon 39 (2001) 425–432.
[50] Z.R. Holan, B. Volesky, Biosorption of lead and nickel by biomass of marine algae, Biotechnol. Bioeng. 43 (1994) 1001–1009.
[51] M.M.D. Zulkali, A.L. Ahmad, N.H. Norulakmal, Oryza sativa L. husk as heavy metal adsorbent: Optimization with lead as model solution, Bioresour. Technol. 97 (2006) 21–25.
[52] C. Cojocaru, G. Zakrzewska-Trznadel, Response surface modeling and optimization of copper removal from aqua solutions using polymer assisted ultrafiltration, J. Membr. Sci. 298 (2007) 56–70.
[53] R. Azargohar, A.K. Dalai, Production of activated carbon from Luscar char: Experimental and modeling studies, Microporous Mesoporous Mater. 85 (2005) 219–225.
[54] D.C. Montgomery, Design and Analysis of Experiments, eighth ed., John Wiley & Sons, New York, NY, 2013.
[55] H. Lata, S. Mor, V.K. Garg, R.K. Gupta, Removal of a dye from simulated wastewater by adsorption using treated parthenium biomass, J. Hazard. Mater. 153 (2008) 213–220.
[56] L. Alidokht, A.R. Khataee, A. Reyhanitabar, S. Oustan, Cr(VI) immobilization process in a Cr-spiked soil by zerovalent iron nanoparticles: Optimization using response surface methodology, Clean Soil Air Water 39 (2011) 633–640.
[57] M.J. Anderson, P.J. Whitcomb, Simplified: RSM. Optimizing Processes Using Response Surface Methods for Design of Experiments, Productivity Press, New York, NY, 2005.
[58] M. Kousha, E. Daneshvar, H. Dopeikar, D. Taghavi, A. Bhatnagar, Box–Behnken design optimization of acid black 1 dye biosorption by different brown macroalgae, Chem. Eng. J. 179 (2012) 158–168.
[59] G.Z. Kyzas, A decolorization technique with spent "Greek Coffee" grounds as zero-cost adsorbents for industrial textile wastewaters, Materials 5 (2012) 2069–2087.
[60] F. Ghorbani, H. Younesi, S.M. Ghasempouri, A.A. Zinatizadeh, M. Amini, A. Daneshi, Application of response surface methodology for optimization of cadmium biosorption in an aqueous solution by *Saccharomyces cerevisiae*, Chem. Eng. J. 145 (2008) 267–275.
[61] S. Mona, A. Kaushik, C.P. Kaushik, Waste biomass of *Nostoc linckia* as adsorbent of crystal violet dye: Optimization based on statistical model, Int. Biodeterior. Biodegrad. 65 (2011) 513–521.
[62] S.L. Ching, M.S. Yusoff, H.A. Aziz, M. Umar, Influence of impregnation ratio on coffee ground activated carbon as landfill leachate adsorbent for removal of total iron and orthophosphate, Desalination 279 (2011) 225–234.
[63] H. Lata, V.K. Garg, R.K. Gupta, Removal of a basic dye from aqueous solution by adsorption using *Parthenium hysterophorus*: An agricultural waste, Dyes Pigm. 74 (2007) 653–658.
[64] I. Langmuir, The adsorption of gases on plane surfaces of glass, mica and platinum, J. Am. Chem. Soc. 40 (1918) 1361–1403.
[65] K.R. Hall, L.C. Eagleton, A. Acrivos, T. Vermeulen, Pore- and solid-diffusion kinetics in fixed-bed adsorption under constant-pattern conditions, Ind. Eng. Chem. Fundam. 5 (1966) 212–223.
[66] H. Freundlich, Ueber die adsorption in Loesungen (Adsorption in solution), Z. Phys. Chem. 57 (1907) 385–470.
[67] M.J. Temkin, V. Pyzhev, Recent modifications to Langmuir isotherms, Acta Physiochim. USSR 12 (1940) 217–222.
[68] C.X.H. Su, T.T. Teng, A.F.M. Alkarkhi, L.W. Low, *Imperata cylindrica* (Cogongrass) as an adsorbent for methylene blue dye removal: Process optimization, Water Air Soil Pollut. 225 (2014) 1941–1952.
[69] G. Annadurai, R.S. Juang, D.J. LEE, Use of cellulose-based wastes for adsorption of dyes from aqueous solutions, J. Hazard. Mater. 92(3) (2002) 263–274.
[70] Y. Bulut, H. Aydın, A kinetics and thermodynamics study of methylene blue adsorption on wheat shells, Desalination 194 (2006) 259–267.
[71] S. Lagergren, About the theory of so called adsorption of soluble substances, kungl. Svenska Vetenskapsakademien. Handlingar, Band 24(4) (1898) 1–39.
[72] Y.S. Ho, G. McKay, Pseudo-second order model for sorption processes, Process Biochem. 34 (1999) v451–465.